World Academy of Science, Engineering and Technology
International Journal of Biomedical and Biological Engineering
Vol:5, No:8, 2011

Multimodal Biometric System Based on Near-Infra-Red Dorsal Hand Geometry and Fingerprints for Single and Whole Hands

Mohamed K. Shahin, Ahmed M. Badawi, and Mohamed E. M. Rasmy

Abstract**—**Prior research evidenced that unimodal biometric systems have several tradeoffs like noisy data, intra-class variations, restricted degrees of freedom, non-universality, spoof attacks, and unacceptable error rates. In order for the biometric system to be more secure and to provide high performance accuracy, more than one form of biometrics are required. Hence, the need arise for multimodal biometrics using combinations of different biometric modalities. This paper introduces a multimodal biometric system (MMBS) based on fusion of whole dorsal hand geometry and fingerprints that acquires right and left (Rt/Lt) near-infra-red (NIR) dorsal hand geometry (HG) shape and (Rt/Lt) index and ring fingerprints (FP). Database of 100 volunteers were acquired using the designed prototype. The acquired images were found to have good quality for all features and patterns extraction to all modalities. HG features based on the hand shape anatomical landmarks were extracted. Robust and fast algorithms for FP minutia points feature extraction and matching were used. Feature vectors that belong to similar biometric traits were fused using feature fusion methodologies. Scores obtained from different biometric trait matchers were fused using the Min-Max transformation-based score fusion technique. Final normalized scores were merged using the sum of scores method to obtain a single decision about the personal identity based on multiple independent sources. High individuality of the fused traits and user acceptability of the designed system along with its experimental high performance biometric measures showed that this MMBS can be considered for med-high security levels biometric identification purposes.

Keywords**—**Unimodal, Multi-Modal, Biometric System, NIR Imaging, Dorsal Hand Geometry, Fingerprint, Whole Hands, Feature Extraction, Feature Fusion, Score Fusion

I. INTRODUCTION

BIOMETRIC devices automate the personal recognition process by association/disassociation of an individual with a previously determined identity/identities. Human biometrics have high uniqueness of physical characteristics such as fingerprints [1]. Biometric devices measure and record these characteristics for automated comparison, identification, and verification purposes.

Mohamed K. Shahin is a PhD Candidate at Systems & Biomedical Engineering Department, Cairo University, Egypt. (phone: 0020100851011; fax: 0020643394355; e-mail: mkhairys@k-space.org).

Ahmed M. Badawi is a professor at Systems & Biomedical Engineering Department (SBME), Cairo University, Egypt. (e-mail: ambadawi@ieee.org). He is a senior member, IEEE.

Mohamed E. M. Rasmy is a professor at Systems & Biomedical Engineering Department (SBME), Cairo University, Egypt. (e-mail: erasmy@gmail.com). He is a life member, IEEE.

Biometric techniques fall into two categories: physiological and behavioral. Common physiological biometrics are face, eye (retina or iris), finger (fingertip, thumb, finger length or pattern), palm (print or topography), hand shape geometry, hand vein patterns, and wrist veins. Common behavioral biometrics include voiceprints, handwritten signatures and keystroke/signature dynamics [2].

Traditionally, biometric systems that use only one biometric trait (unimodal biometric systems) were very common. Almost a decade ago, many drawbacks appeared in these unimodal systems like: Noise in the acquired features, Intra-class variations, Inter-class similarities [3], Non-universality, and Spoof attacks [4]. Recently, some MMBSs were reviewed and successfully developed to significantly overcome some of these problems [2], [4]-[32]. These systems were proposed to fulfill the need for better recognition accuracy by consolidating more than one independent source of evidences to recognize identities. Moreover, the MMBS may ensure that a living person is there at the gate by asking the person to enter a random sequence of his/her biometric traits [4]. Finally, biometric system design is all about 2 major characteristics, the first is the individuality of the patterns used by the system and the second is the usability and user acceptability by persons, by society, or by culture.

A. Prior Related Work

Ross *et al.* [4] discussed various scenarios that can be possible in MMBS, levels of fusion that are plausible and integration strategies that can be used for information consolidation and how we can get benefits from multiple sources of biometric information that MMBS provides to get an identity decision. Multimodal biometric systems can take different forms depending on how they gain the multiple source of information: (a) Multi-sensor systems: a single biometric trait is imaged using multiple sensors in order to extract diverse information from the acquired images, e.g. a system may fuse the FP information of a user obtained using an optical and a capacitive FP sensors. (b) Multi-algorithm systems: the same biometric data is processed using multiple algorithms, e.g., a texture-based algorithm and a minutiae-based algorithm can operate on the same FP image in order to extract different feature sets that can improve the performance of the system [20]. (c) Multi-instance systems: these systems use multiple instances of the same body trait. For example, the right index and ring FPs of an individual may be used to verify

an individual's identity [26]. (d) Multi-sample systems: a single sensor may be used to acquire multiple samples of the same biometric trait in order to account for the variations that can occur in the trait, or to obtain a more complete representation of the underlying trait. A FP system equipped with a small size sensor may acquire multiple partial prints of an individual's finger in order to obtain images of various regions of the FP. A mosaicing algorithm may then be used to concatenate the multiple impressions and create a larger FP image [14]. (e) Multimodal systems: these systems combine the evidence presented by different body traits for establishing identity. Physically uncorrected traits (e.g., FPs and HGs) [26] are expected to result in better improvement in performance than the correlated traits (e.g. voice and lip movement).

For achieving high recognition ability by MMBS, intelligent and effective fusion methodologies must be applied throughout the system different stages. One can consider each single biometric modality as a single expert window and the main rule of the fusion strategy is to combine all of these windows together into a single decision of the identity. The fusion can be applied at several levels through the biometric system steps and we can classify fusion strategies into 2 basic categories: (a) Fusion before matching, such as sensor-level fusion [14] and feature-level fusion [23], and (b) Fusion after matching such as matching score-level fusion [10], rank-level fusion [9], and decision-level fusion [15]. The former categorization was done based on the fact that information available is substantially reduced after the matching process took place [9], [11].

Rowe *et al.* [24] proposed a multimodal system based on hand shape, fingerprints and palmprint, the advantage of the proposed system is the use of a single sensor for acquiring the three modalities but they tested their proposed system using a medium-size database of 50 volunteers, they achieved a GAR of 91.5% at FAR of 0.01% by fusing the palmprints from 2 hands using the product rule. Kumar et al. [16], [18] proposed a system based on feature selection of hand geometry and palmprint, and used the Discrete Cosine Transform (DCT) coefficients for palmprint recognition. They used the Correlation-based Feature Selection (CFS) to select the dominant feature set for both HG and palmprint. Other MMBS for the same group [17] that is based on combining fingerprint, palmprint, and hand-shape was proposed. Their proposed acquisition system is able to image only the hand shapes from which they extracted a region containing the palmprint information. Finally, they added a generic random fingerprints database to their 100 persons right hand shapes dataset collected by their prototype, they reported an EER of 3.53%.

Wei *et al.* [30] presented another MMBS based on palmprint and hand geometry. They tested their MMBS using an experimental dataset of 51 persons with a reported accuracy of 99.36% for the fused 2 modalities. Wu *et al.* [31] fused the phase and orientation information of the palmprint in order to authenticate identities. They tested their MMBS using data set of 392 persons with a reported good accuracy enhancement of EER of 0.31%. Zhu *et al.* [32] proposed a MMBS based on finger geometry, knuckle print, and palmprint. They imaged the front surface of the hand shape using a webcam for 190 subjects. They used a decision-level fusion scheme based on the simple AND-rule, with a high performance results for FRR of 0.00898% at FAR of 2.52e-6%.

Cui *et al.* [5] introduced a MMBS based on feature merging, selection, and fusion applied to face and iris images. They recognized the identities based on Nearest Neighbor Decision rule. They concatenated 2 small public single-modality face and iris datasets of 40 persons to test their MMBS, with a reported recognition accuracy for random choose training and testing samples ranging from 88.7% to 100%. Snelick *et al.* [28] developed a MMBS for face and fingerprint, with fusion methods at the score level where 3 FP and one face commercial systems were used in their study. They tested 7 different score normalization techniques and 5 different fusion methods. Their best EER of 0.63% was reported when the max-score fusion approach on quadric-linequadric normalized scores was used.

Monwar *et al.* [9] attempted to alleviate the unimodal biometric system tradeoffs combining physiological and behavioral traits by proposing a MMBS based on face, ear, and signature. They fused the evidences based on rank level integration strategy for testing the proposed system via collecting and pairing public domain unimodal biometric databases into a virtual multimodal dataset of 40 persons with performance enhancement of 1.12% EER. The merit of system in [9] is its combining physical and behavioral traits while disadvantages are low database size used and the different unimodalities are virtual and do not belong to the same persons.

Sim *et al.* [27] proposed a framework for fusing the face and fingerprints for continuous monitoring of the presence of only legitimate users into the secured rooms. They installed a system of Canon VCC4 video camera and a SecureGen mouse that contains a sweep FP sensor on a PC for continuously monitoring the person who accessing the secure resources. They captured 1000 FP images and 500 Face images from several users to train their system. They achieved a good performance by the fusion in a tradeoff between usability and probability of time to correct reject (PTCR) which is analogous to the FAR-FRR tradeoff.

Nandakumar *et al.* [20] proposed a minutiae and texture based fingerprint fusion study using a quality-weighted sum (QWS) rule for score level fusion, with an achieved EER of 3.39% on a subset of the MCYT FP database [33] of 750 fingerprints belonging to 75 persons. Nadakumar *et al.* [19] addressed the shortage or missing data (modalities or incomplete score lists) during solving the identity searching problems within a large multimodal databases. They developed a fusion scheme specifically for the identification mode that can handle partial data without any need for rules design on a case-by-case basis.

The majority of multimodal systems and studies recently proposed in the literature suffer from several drawbacks like: (a) The proposed MMBS were tested and validated on a small to medium size datasets around 50 persons. (b) The datasets used to measure these MMBS performance are originally a

unimodal biometric databases collected from different public domain areas and were added to form a multimodal datasets, i.e. a virtual database which contains records created by consistently pairing a user from one unimodal database (e.g., face) with a user from another database (e.g., iris) [5], [9], [12], [17]. (c) Lack of simple and compact multimodal acquisition prototype for dedicated interacting and user convenience while acquiring multiple unique traits in just one or two simple steps. (d) MMBS is about having increased performance accuracy and most of reviewed systems have not achieved enough accuracy increase by the fusion of uni-modalities. (e) Lack of getting complete benefit from the sensors capabilities (i.e. acquiring the right hand shapes only as in most research and commercial hand geometry devices instead of acquiring both hands shape).

B. Biometric System Performance Comparison

The most important enhancement for any MMBS is to show higher accuracy versus its constituents of single-modality biometric systems. In addition to the measures of system imposter rates like: FAR (FMR), and FRR (FNMR) [29], [34], we compared our proposed systems performances using qualitative and quantitative approaches. The *qualitative* measures are graphs to show the system performance within a range of thresholds. Example is the total biometric system accuracy versus a range of thresholds (as in Fig. 8 and Fig. 13 of [35]). The accuracy can be calculated at each threshold as:

$$Accuracy\ (\%) = \frac{GA+GR}{GA+FR+GR+FA}\ x\ 100(\%) \quad (1)$$

The accuracy parameter measures the percentage of genuine (G) events to all the genuine and false (F) events (G+F). Furthermore, the point of maximum accuracy can be considered as the operating point at which we can compare the genuine and false rates of different biometric systems. The performance of biometric systems can be summarized using the Receiver Operating Characteristic curves (ROCs) [36]. ROCs plot the Genuine Accept Rate (GAR) versus False Accept Rate (FAR) on a semi-logarithmic curves (as illustrated in Fig. 9). The quantitative measures we used are the EER [11] and TER [29]. The EER refers to the point at which the FAR equals the FRR during the performance testing (as shown in Fig. 13). We also calculated the TER, which equals $\min(\text{FAR} + \text{FRR})$. EER is sometimes approximated by ~TER/2 at optimal threshold and minimization of EER may be treated as minimization of TER [21], [29]. In our analysis we calculated both EER and TER measures independently.

C. Proposed MMBS Objectives and Paper Organization

In this paper, we introduce our MMBS based on single or both hands using NIR dorsal hand geometry (HG) and fingerprint (FP) modalities. The proposed system was designed to tackle the tradeoffs of the current unimodal and some MMBSs explained earlier. The system was tested using an experimental multimodal database of 100 persons of which HG and FP were acquired and collected from the same persons using the prototype design proposed in 2008 [26].

Our multimodal biometric prototype system acquires Rt/Lt index and ring FP, Rt/Lt Near-Infra-Red (NIR) dorsal hand geometry shape (HG), Rt/Lt NIR dorsal hand vein (HV) tree patterns *in just a single user maneuver*. It captures Lt index and ring FP with Lt HG shape and Rt HV pattern, in a single step or captures Rt index and ring FP with Rt HG shape and Lt HV pattern, in a second step. Our proposed prototype hardware unit can be designed with a dedicated H/W for standalone systems.

One major advantage of adding the NIR HG/HV patterns is its good detection of liveness as explained in [26]. The other advantage of using thermal signals for HG/HV is that, it can only be detected using a NIR camera (hand shapes and hand veins are thermal sources to these cameras), and are hard to fake using the standard techniques [37]-[38]. In this paper, we are presenting the experimental results of single and both hands HG and FP MMBS only. The proposed system can be considered for multimodal authentication and identification purposes with some advantages over few existing multimodal systems as explained in [26].

This paper is organized as follows, section I introduces MMBS, gives brief idea about its prior research work, and illustrates the paper objectives and organization. Section II describes detailed prototype design for our multimodal acquisition prototype. Section III presents HG feature extraction process, estimates the probability of true match between Rt and Lt HG pattern for the same person, and introduces our Rt-Lt-HG biometric system. Section IV gives an idea about FP image enhancement, minutiae points extraction, and minutiae graph matching. Also, introduces our multi-instance Rt-Lt-FP biometric system. Section V introduces fusion of HG and FP using a score-level fusion technique and presents 3 MMBSs: Rt-HG-FP, Lt-HG-FP, and Rt-Lt-HG-FP, respectively. Section VI gives discussion of the proposed MMBS merits and performance and our planned objectives for the system. Finally, section VII concludes this paper.

II. MULTIMODAL BIOMETRICS PROTOTYPE DESIGN AND DATA ACQUISITION

A. Prototype System Design

In order to design a setup for acquiring 3 biometric modalities (HG, FP, and HV) for achieving our proposed MMBS objectives; we set our plan to image the landed freestyle hand for obtaining the NIR HG shape and FP images at the same time in one acquisition step for either right or left hands. The left compartment shown in Fig. 1, was designed to acquire both the landed freestyle NIR HG shape [39] and the FP for the index and ring fingers [26], using USB interface (similar to our single finger acquisition [40]). The right compartment shown in Fig. 1 was designed to image the back of the hand as a clenched fist, for imaging the NIR HV. The right compartment is considered for near future acquisition

and beyond this paper objective, we have presented the preliminary images acquired for the three modalities (FP, HG, and HV) in [26]. Fig. 1 (left) shows how to use our MMBS prototype. Our prototype system unit was designed to image both Rt and Lt hands for the 3 modalities (FP, HG, and HV).

In FP module design, we used the FPS200 Solid-State Capacitance FP sensor chip; manufactured by Veridicom International Inc. Company [41] to acquire the FP images. Advantages of capacitive FP sensors are its very compact and miniaturized size and low price. Its only limitation is its short durability for continuous use (~9-12 months). In order to acquire 2 FP images and the HG shape at the same time, we designed a PCB for soldering 2 FP sensors and attached the PCB in front of the hand shape NIR CCD imager. Fig. 2 shows our PCB design with the 2 sensors and its USB interface. The subject's index and ring fingers can fit on the sensors while the hand is fully landing to permit the dorsal HG shape to be acquired at the same time. The 2 FP sensors were interfaced to the PC using the USB bus [26], [42]. The output image array size is 300X300 pixels with 500 dpi spatial resolution.

Fig. 1. Multimodal Biometric Prototype acquisition: the left compartment is for HG and FP and the right one is for the HV

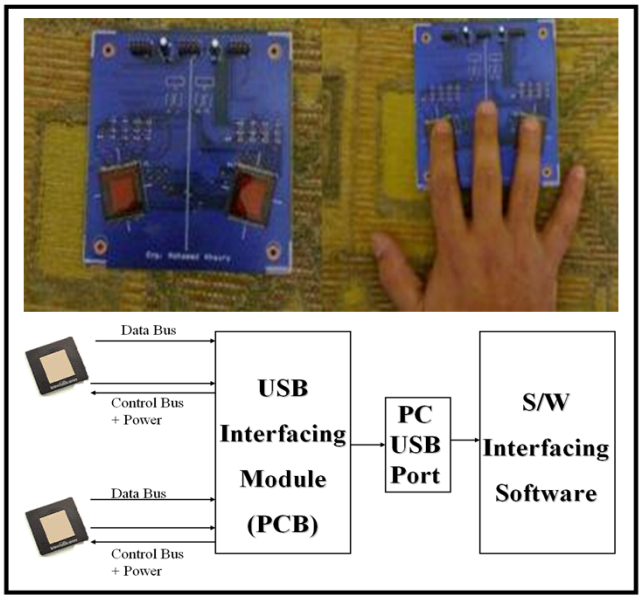

Fig. 2. Two FP capacitance sensors installed on a single PCB to acquire both Index and Ring FP (top) and its USB interface (bottom)

For capturing the NIR HG shape, we installed NIR CCD camera along with external NIR LEDs, all in the center of the left compartment top. The CCD video signal was captured using a low cost standard video frame grabber. We used the 2 capacitive FP sensors as markers to let the users normally center their opened-fingers Rt/Lt hands on the left compartment platen and to give the opportunity for the FP sensors to capture the index and ring FPs at the same time [26].

B. Prototype Acquisition Results and Image Quality

In this section, we show the good quality acquired images, Fig. 3 shows samples of the acquired multimodal database for HG and FP (HV samples can be found in [26], [34]-[35], [46]-[47]). Fig. 3 (1,2) shows a high quality NIR HG sharp edges with high contrast between hand and background platen (High contrast due to our well designed external cold source IR LEDs and contrast light absorbing platen). These acquired images are very suitable for the geometry and shape dimensions measurement. The FP images in Fig. 3 (3-6) show a medium to high quality FP images. We extracted the FP feature points (minutiae), the matching process will be accomplished via a graph point-matching algorithm using the extracted minutia points.

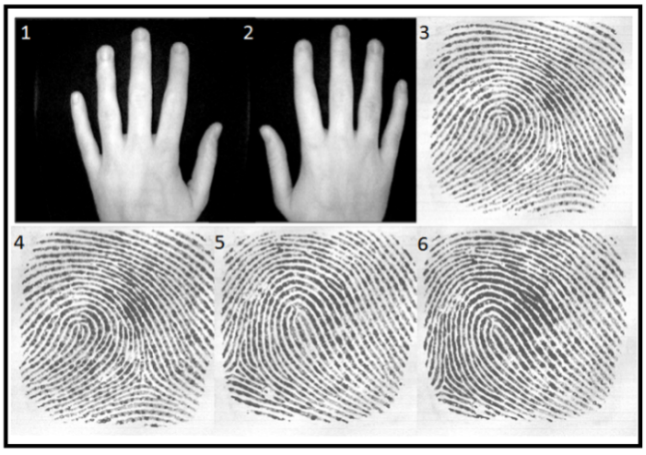

Fig. 3 Acquired sample images from the hand shape imager for Rt/Lt hands, (1,2). Sample images from the Lt FP sensor (Rt Index FP), (3,4). Sample images from the Rt FP sensor (Rt Ring FP), (5,6)

C. Database Collection Protocol

We had a written consent from all volunteers consistent with IRB, where we explained and read a verbal agreement of the purpose of study (no subjects interaction and FP sensors and boards were cleaned from one volunteer to others regarding hygienic factors), to each volunteer and let them sign the consent, all coauthors were also volunteers in database. We captured a new multimodal database of 100 different volunteers of ages from 15-70, and from different working conditions, for the proposed multimodalities of FP and NIR HG shape (and we are currently acquiring HV images to same volunteers). Volunteers were just asked to

place their hands in a none controlled fashion (no training), just opening their non-touching fingers normally at any angles for geometry acquisitions, and pointing their index and ring fingers to be on the well designed and oriented fingerprint sensors installed over the platen in left compartment (the distance and rotation between the 2 sensors were empirically designed to fit all persons of different ages, sexes and hand sizes) [26]. All volunteers were healthy (no arthritis, no hands or finger cuts, may have scars in their fingerprints) and from different working conditions. Images were captured through 5 days intervals for each volunteer from 2008 till 2010 in a fully non-controlled environment (volunteers were not trained on using the system prior to their data acquisition and this allows for normal angulations between non-touching fingers).

We acquired 5 images for each modality for both right and left hands (right NIR HG, left NIR HG, right index FP, right ring FP, left index FP, left ring FP,) at different time intervals, and at different conditions. The system acquisition is a whole-hands system, number of images of 20 (Rt/Lt, Index and Ring) FP, and 10 Rt/Lt HG images were acquired for the performance study and fusion analysis. A total of 30 acquisitions were captured from each volunteer, for 100 volunteers. A total of 3000 images were in our database. HG images acquired in 240X320 pixels with a spatial resolution of 72 dpi NIR HG shape. FP resolution for the used Veridicom sensors is a 500 dpi, the image size is 300X300 pixels. Our processing software is efficiently custom designed in MS VC++, and MathWorks MatLab. Raw images were stored with no compression, to keep the highest quality possible for future analysis [26].

III. HAND GEOMETRY FEATURE EXTRACTION, MATCHING, AND FUSION

A. HG Image Processing and Feature Extraction

As we discussed in the previous section, we used our proposed setup [26] to acquire persons hand shapes. The hand shape and FPs were imaged while it is landed on the platen. As the FP sensors were in the image background, in order to remove the Veridicom chip borders from the image, platen was painted in a light absorbing black material paint and the chips were slightly below platen so that both index and ring are being parallel to the platen as other fingers. Each volunteer provided 10 different hand shape images in our database (5 for Lt and 5 for Rt), we constructed a data set of 1000 different HG images belonging to 100 persons. 2D images of the hand were processed as in the flowchart shown in Fig. 4 [26], [39], [43-45]. This method performs multiple preprocessing steps to form a contour of the hand. The contour can then be converted into polar coordinates in order to determine the 5 maxima (finger tips) and 4 minima (finger valleys) of the hand. From this information, a total of 44 points hand model can be determined, as shown in Fig. 5 up. A total of 29 geometric features of the hand and fingers were extracted using these points, including 14 widths, 5 lengths, 5 circumferences, and 5 square root areas of the different fingers.

In this study, we proposed an automatic algorithm to differentiate between the Rt and Lt hand type using the idea of Euclidian distances comparison illustrated in Fig. 5 bottom, where from the intuitive fingers dimensions and normal minimum-maximum fingers opening, distances (D4 and D2) cannot be changed a lot due to anatomical (muscular and bony) limited mobility constraints on the carpal and metacarpal bones; unlike distances (D1 and D3) which are of more mobility and usually with normal opening D1>D2 and D3>D4. In our HG features extraction module, if we encountered a Lt hand shape, we just flip the order of the polar coordinates array, and the maxima-minima array, and we continue to calculate the HG geometric features exactly as what we do for any Rt hand shape (it is a mirror transform). The identity is positive if the Euclidian distance between the stored feature template "F" and the claimed identity "Y" is less than a threshold value “T” as in (2):

$$\sqrt{\sum_{i=1}^{d}(y_i - f_i)^2} < T \qquad (2)$$

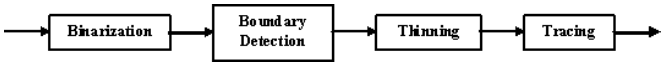

Fig. 4 Hand shape image processing steps

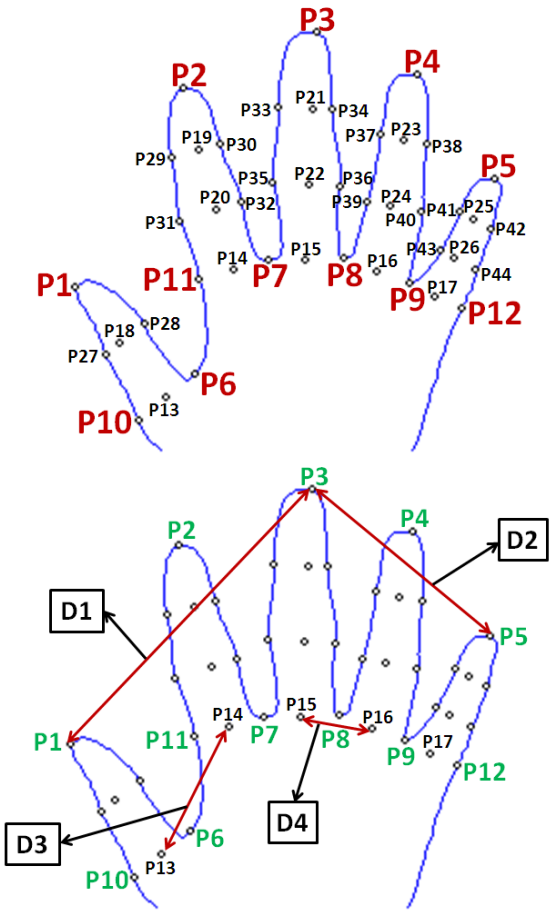

Fig. 5 Automatically detected 44 point hand model (P1-P5 Maximas, P6-P9 Minimas), (Up). Rt/Lt automatic hand type differentiation algorithm: If (D1 > D2) AND/OR (D3 > D4) then image is for Rt HG, otherwise image is for Lt HG, (Bottom)

B. Estimating the Probability of True Match Between Rt and Lt HG Pattern Similarity for Same Person

For calculating the probability for a true-match between Rt and Lt HG patterns for the same person, we manipulated each hand shape as a separate and independent HG pattern (i.e. 5 Rt hand images are different from 5 Lt hand images for the same person), *as if* we have a database of 200 persons each person has 5 different scenes. We constructed the distance matrix for representing the matching result between each image and all other images. The distance matrix is filled with the *matching distances* between the image defined by the row label versus the image defined by the column label, so its width and height are 1000 elements each (a million matches). We calculated the probability for the matching distance to be less than or equal to the threshold that the maximum system accuracy occurred at [35]. Table I shows the probability values for the thresholds range from 0.01 to 0.02. From Table I, The probability of similarity between Lt-HG and Rt-HG at the threshold that gave us the maximum accuracy (which was 0.017) was: P(Matching Distance <= 0.017) = 11.31%. The probability is high enough to conclude that the HG pattern is unique for each identity, but is not unique for each hand i.e. the HG for the Rt hand is similar to some extent to the HG pattern (defined by our 29 features dimensionality) for the Lt hand for the same subject.

TABLE I
RESULTS FOR THE PROBABILITY FOR THE TRUE MATCH BETWEEN THE RT/LT HG PATTERNS FOR THE SAME IDENTITY WITH MEAN = 0.27648 AND STD. DEV. = 0.008805243.

Threshold	Z-score	P(Z)	0.5 - P(Z)	P(Distance <= Threshold)
0.01	-2.00428	0.4772	0.0228	2.28%
0.011	-1.89071	0.4706	0.0294	2.94%
0.012	-1.77714	0.4625	0.0375	3.75%
0.013	-1.66358	0.4525	0.0475	4.75%
0.014	-1.55001	0.4394	0.0606	6.06%
0.015	-1.43644	0.4251	0.0749	7.49%
0.016	-1.32287	0.4066	0.0934	9.34%
0.017	**-1.209**	**0.3869**	**0.1131**	**11.31%**
0.018	-1.09573	0.3643	0.1357	13.57%
0.019	-0.98216	0.3365	0.1635	16.35%
0.02	-0.86859	0.3078	0.1922	19.22%

C. Bi-Instance Biometric Systems Based on Hand Geometry Feature and Score Fusion

We constructed 3 bi-instance HG biometric systems, the first one based on feature-level fusion of Lt-HG and Rt-HG feature vectors, the second one based on Lt-HG and Rt-HG score-level fusion using the multiply-of-scores method, and finally the third one based on Lt-HG and Rt-HG score-level fusion using the sum-of-scores technique. In order to encode the Rt and Lt HG patterns in one array (feature fuse Lt-HG with Rt-HG) that represents one identity, the 2 arrays which represent Lt-HG and Rt-HG measurements features were *concatenated* (fused) into a single feature vector of dimension 1X58 that completely represents the whole hands HG shape. We constructed a bi-instance HG biometric system based on feature-level fusion (as shown in Fig. 6). Our HG data set consists of 100 persons; each person enrolled his/her Lt and Rt 5 times, the distance matrix width and height were 500X500 elements (a 250000 matches).

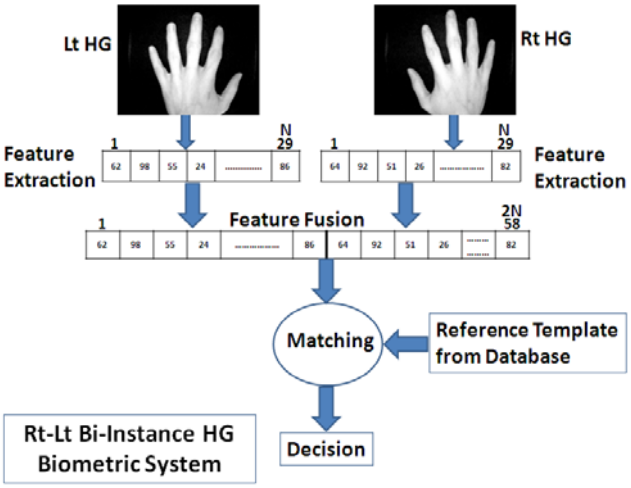

Fig. 6 Rt-Lt-HG (Feature-Level fusion) bi-instance biometric system schematic

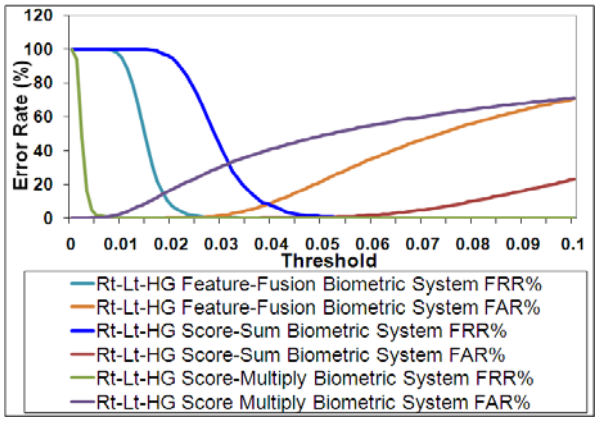

Fig. 7 FAR versus FRR and EER for our Rt-Lt-HG bi-instance biometric systems

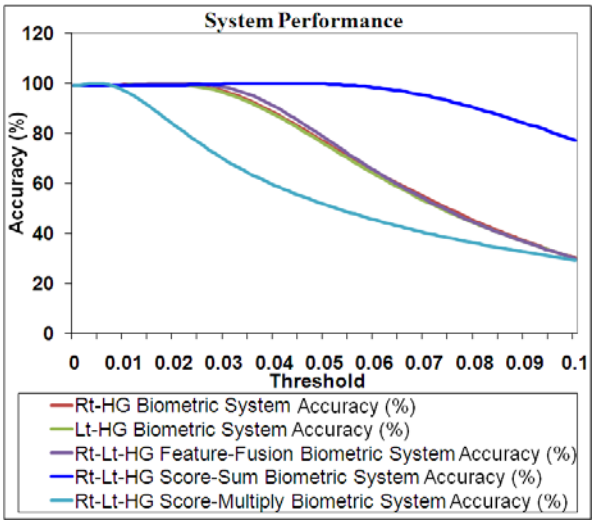

Fig. 8 Accuracy for our HG single-modality and bi-instance biometric systems

We fused the output of Lt-HG and Rt-HG single-experts on the score-level using both the multiply-rule and the sum-rule. We plotted FAR-FRR, accuracy, ROC curves, and genuine-imposter distribution curves for the single-modality HG biometric systems (Lt-HG & Rt-HG), and after HG features and scores fusion (Rt-Lt-HG bi-instance biometric systems), all are shown in Figs. 7-10. Since we achieved slight higher quantitative accuracy results using the HG feature-level fusion technique as seen from Table II, we will continue using the HG feature fusion.

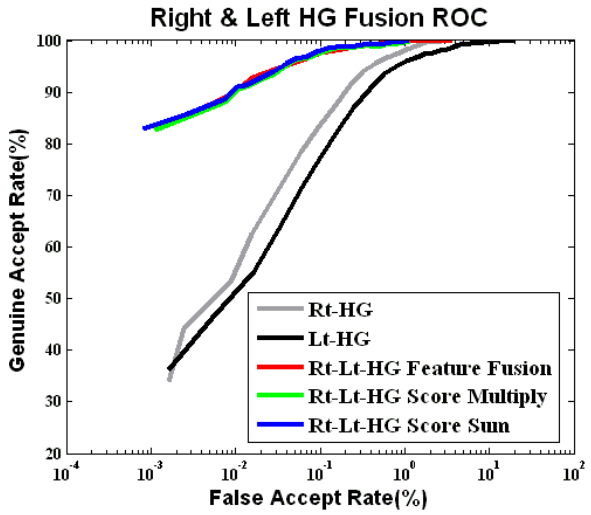

Fig. 9 ROC curves for Rt-HG, Lt-HG, bi-instance Rt-Lt-HG (Feature-Level Fusion), bi-instance Rt-Lt-HG (Score-Level Fusion using Score-Multiply and Score-Sum Rules) biometric systems

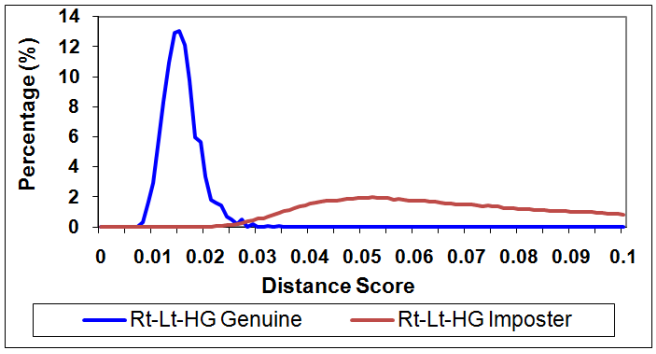

Fig. 10 Genuine and imposter distance score distributions for Rt-Lt-HG (Feature-Level Fusion) bi-instance biometric system

IV. FINGERPRINT FEATURE EXTRACTION, MATCHING, AND FUSION

A. FP Image Enhancement and Feature Extraction

For detecting the FP ridge ends and bifurcations features, Short Time Fourier transform (STFT) was used to enhance the FP image using the frequency and the direction of the ridges [48]. The ridges frequency and direction were calculated locally in the frequency (Fourier) domain. Image was enhanced using a directional bandpass filter in the frequency spectrum.

We used a technique called MINDTCT (Minutiae Detection) published by the National Institute of Standards and Technology (NIST) for extracting the minutiae points (ridge endings, and bifurcations) from the enhanced FP images [49]. The algorithm captures the enhanced gray scale FP images, generates a block level directional map (assigns one direction for each 8X8 block of the FP image), uses the directional map to directionally binarize the image, extracts the FP minutiae directly from the binary image using set of predefined templates, and finally removes the false minutiae from the initial extracted feature list using set of post-processing algorithms. Fig. 11 shows the results of applying these algorithms to a random sample from our acquired FP images. Enhanced images showed very high quality and a successful features extraction for all our acquired FP images.

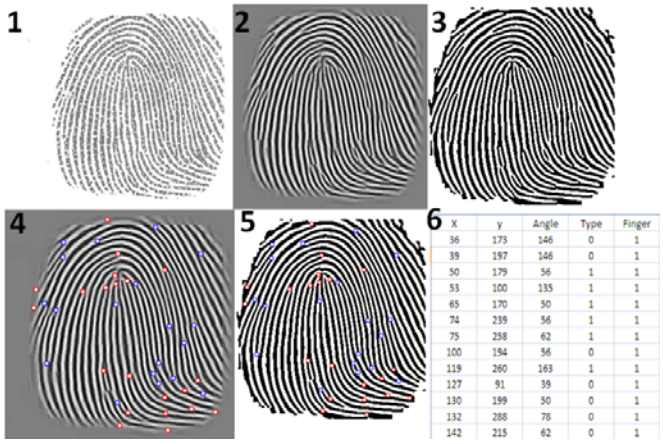

Fig. 11 Original FP image (1), enhanced image (2), binary image (3), extracted minutiae superimposed on the enhanced image (4), extracted minutiae superimposed on the binary image (5), extracted minutiae feature file example (6)

B. Graph Matching and Our Proposed Fingerprint Feature Fusion Method

We represented each minutia point with 5 parameters (X, Y, Θ, Type, FingerCode), X: is the horizontal coordinate, Y: is the vertical coordinate, Θ: indicates the orientation angle, Type: determines the type (0: ridge ending, 1: ridge bifurcation), FingerCode: indicates from which finger this minutia was originated (1: right ring, 2: right index, 3: left index, 4: left ring), we used FingerCodes field for FP feature fusion, as illustrated below. The example output minutiae file is shown in Fig. 11(6). Clearly, The FP matching relies mainly on robust feature extraction which is dependent on the quality of images. The matching algorithm takes template and reference representations (R, T) of two single or fused fingerprints and returns a single similarity score S(R,T) that can be generated using a very popular approach [7] as in (3):

$$S(R,T) = \frac{m}{\min(M_R, M_T)} \quad (3)$$

where *m* represents the number of matched minutiae, M_R and M_T represent the number of minutiae in the reference and template prints, respectively.

We used a graph based minutia points matching algorithm [50] for robust fingerprint recognition. The algorithm uses the local matching to consolidate and relate minutia points with their neighbors, so it accounts for nonlinear transformation of minutia points since only the local neighbor points are matched at each stage. The algorithm introduced a new representation called K-plets for representing each minutia point with its neighbor points. The graph constructed by looking for 4 neighbors for each minutia point, one nearest neighbor in each of the 4 quadrants sequentially, so the matches can propagates in all directions of the fingerprint pattern. When we fused fingerprints that originated from different fingers for the same person in one feature vectors, we concatenated the files containing the minutia points parameters.

We matched the fused fingerprints using a single matcher as follows. We analyze the input minutia feature files. If we found more than 1 FingerCode (i.e. 2 or 4 different FingerCodes), it means that this file contains minutia points from more than single finger for the same user. We looked for more than 1 matched graph within the reference and template minutia patterns (i.e. 2 or 4 matched graphs). Finally, we searched for largest graph within the minutia points that have the same FingerCode preventing the matcher from aligning any two minutia points which originates from different fingers (i.e. have different FingerCode) together in one graph.

C. Bi-Instance and Multi-Instance Biometric Systems Based on Fingerprints Feature and Score Fusion

The No. of minutia points that represent the uniqueness is variable for each FP, with min., max., and avg. of 21, 74, and 44.79 points, respectively over all of our 2000 fingerprints. We constructed 10 fingerprint biometric systems: 4 are single-modality FP (Rt-Ring, Rt-Index, Lt-Index, and Lt-Ring), 2 are bi-instance FP (Rt-FP, and Lt-FP) using our FP feature-level fusion technique, 2 are bi-instance FP (Rt-FP, and Lt-FP) using the sum-of-scores score-level fusion method, the 9th is a multi-instance FP (Rt-Lt-FP) biometric system using our minutiae feature-level fusion scheme (as shown in Fig. 12), and finally the 10th is a multi-instance FP (Rt-Lt-FP) biometric system using sum-of-scores score-level fusion method. We matched the fused minutia vectors from 2 or 4 different FPs that belong to same person. The similarity score for the fused FP feature vectors $S(R_1, R_2, \dots, R_n, T_1, T_2, \dots, T_n)$ can be generated by a general form of (3) as in (4):

$$S(R_1, R_2, \dots R_n, T_1, T_2, \dots, T_n) = \frac{\sum_{i=1}^{n} m_i}{\sum_{i=1}^{n} min\,(M_{R_i}, M_{T_i})} \quad (4)$$

where M_{R_i} and M_{T_i} are the No. of minutiae that have the same FingerCode, *i*, within the reference and template input feature, respectively, which yielded a matched graph with a minutiae count equals to m_i, and *n* is the No. of fused fingerprints.

We constructed 10 different matching matrices, one for each of 10 FP biometric systems, each matching matrix width and height were 500 elements (a 250000 matches) for each of the 10 systems. From each matching matrix, we deduced EER, TER and the maximum system accuracy. Also, we had a qualitative graphical comparisons between the performance and accuracy of the single-modality FP biometric systems, and after we performed both the FP minutiae feature fusion and score-level fusion using the sum-of-scores technique (Rt-FP, Lt-FP, and Rt-Lt-FP as a bi- and multi-instance FP biometric systems), as shown in Figs. 13-16. Since we achieved slight higher accuracy results using our FP feature-level fusion methodology as seen from Table II, we will continue throughout this paper using our FP feature fusion schemes.

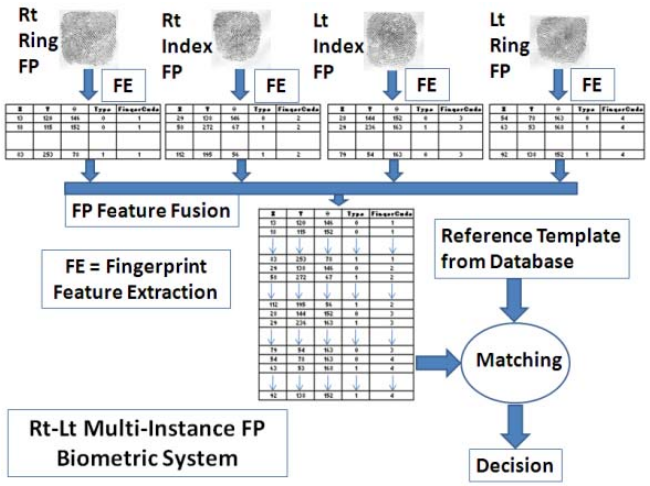

Fig. 12 Rt-Lt-FP (based on minutiae feature fusion) biometric system

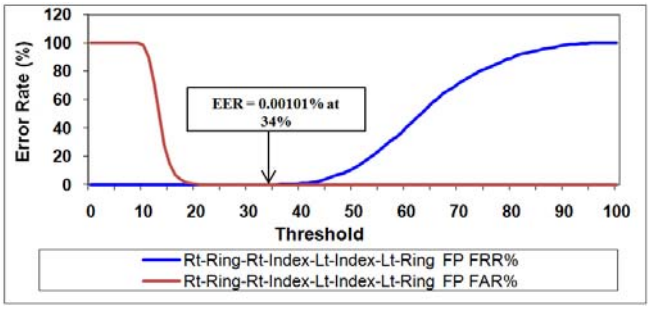

Fig. 13 FAR versus FRR and extracted EER for Rt- Lt (using our minutiae feature fusion scheme) multi-instance FP system

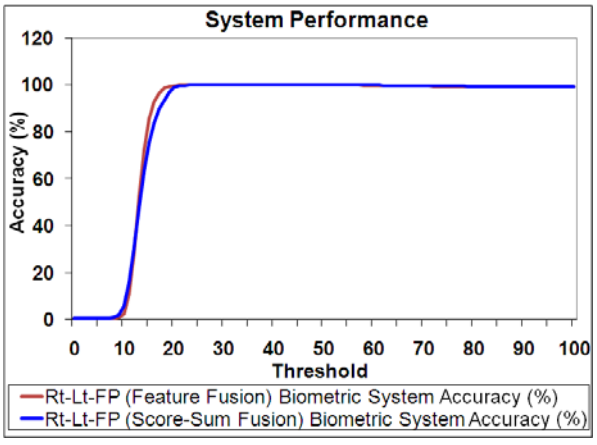

Fig. 14 Accuracy for our Rt-Lt multi-instance FP systems

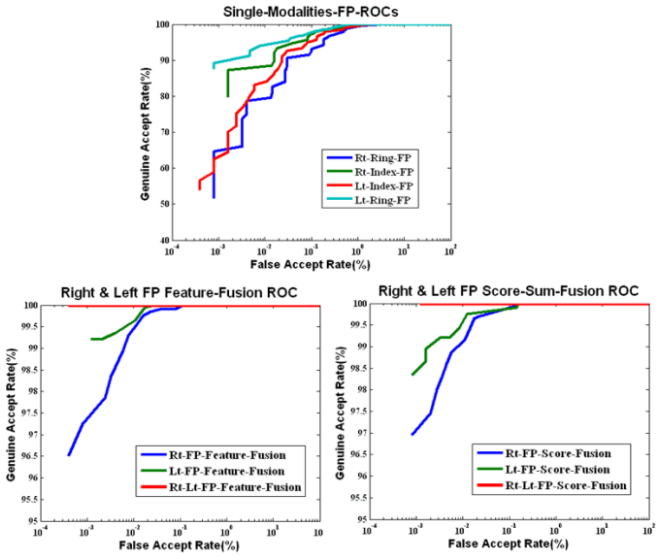

Fig. 15 ROC curves for the 4 single-modality (up), ROC curves for the 3 bi- and multi-instance (using our FP feature-level fusion method) (bottom left), and ROC curves for the 3 bi- and multi-instance (using sum-of-scores score-level fusion technique) FP biometric systems (bottom right)

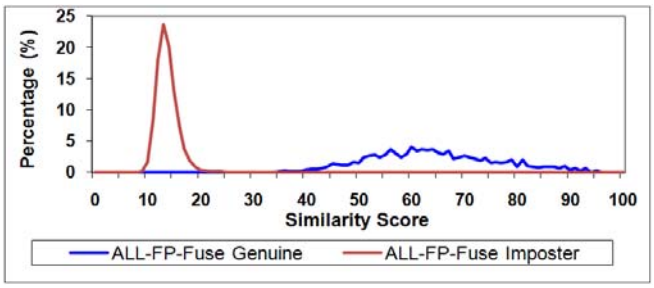

Fig. 16 Identification test for genuine and imposter similarity score distributions of multi-instance Rt-Lt-FP biometric system using our minutiae feature fusion scheme

V. HAND GEOMETRY AND FINGERPRINT MATCHING SCORES NORMALIZATION AND SCORE FUSION

Score normalization refers to changing the location and scale parameters of the match score distributions of the individual matchers, so that the match scores of different matchers are transformed into a common domain [11].

Many techniques can be used for score normalization such as Min-Max, Decimal-Scaling, Z-Score, Median, Median Absolute Deviation (MAD), Double Sigmoid Function, Tanh-Estimators, Bayes based, or piecewise- linear [22]. We used the Min-Max normalization technique. Min-Max normalization is best suited for the case where the bounds (maximum and minimum values) of the scores produced by a matcher are known. Min-Max normalization retains the original distribution of scores except for a scaling factor and transforms all the scores into a common range [0,1]. Distance scores can be transformed into similarity scores by subtracting the normalized score from 1 [11]. Let s_j^i denote the i^{th} match score output by the j^{th} matcher, i = 1,2,..., N; j = 1, 2 , . . . , M (M is the number of matchers and N is the number of match scores available in the training set). The Min-Max normalized score, $n\_s_j^t$, for the test score s_j^t is given by:

$$n\_s_j^t = \frac{s_j^t - \min_{i=1}^{N} s_j^i}{\max_{i=1}^{N} s_j^i - \min_{i=1}^{N} s_j^i} \quad (5)$$

Several methods can be implemented for merging and fusing the normalized scores like max-score, min-score, sum-of-scores [11]. In this work, we fused the scores using the score-sum method. The sum of score, n_s, for N normalized scores, $n\_s_1, n\_s_2, \ldots\ldots, n\_s_N$ is given by:

$$n\_s = \frac{\sum_{i=1}^{N} n\_s_i}{N} \quad (6)$$

Using the Min-Max score-normalization technique and the score-sum fusion methodology, we constructed 3 multimodal HG-FP biometric systems that resulted from HG and FP score fusion of 100 persons. Firstly, Rt-HG-FP MMBS which resulted from fusing the Rt-HG, Rt-Ring-FP and Rt-Index-FP patterns. The following subsection "A" illustrates the Rt-HG-FP MMBS schematic and results. Fig. 17 shows the schematic of Rt-HG-FP multimodal system, Figs. 18-20 qualitatively compare the systems performance between Rt-HG-FP multimodal system and its constituents of Rt single-modality biometric systems. Secondly, the Lt-HG-FP MMBS which resulted from fusing the Lt-HG, Lt-Index-FP, and Rt-Ring-FP patterns. Subsection "B" illustrates the Lt-HG-FP MMBS construction and results. Fig. 17 shows the schematic of Lt-HG-FP multimodal system, Figs. 21-23 qualitatively compare the systems performance between Lt-HG-FP multimodal system and its constituents. Finally, the Rt-Lt-HG-FP MMBS which resulted from fusing the Rt-HG, Lt-HG, Rt-Ring-FP, Rt-Index-FP, Lt-Index-FP, and Rt-Ring-FP patterns. Subsection "C" illustrates the Rt-Lt-HG-FP MMBS construction and results. Fig. 24 shows the schematic of Rt-Lt-HG-FP multimodal system, Figs. 25-28 qualitatively compare the systems performance difference between Rt-Lt-HG-FP multimodal system and its constituents. Table II gives a quantitative performance comparison of all systems based on EER and TER.

A. Rt-HG-FP Multimodal Biometric System

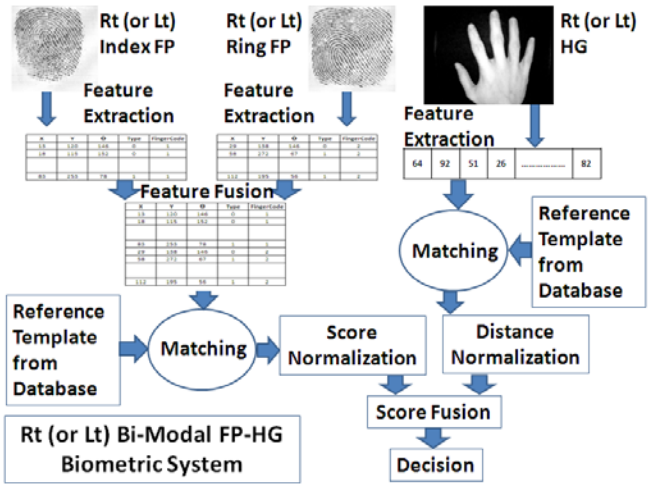

Fig. 17 Schematic for Rt-HG-FP (or Lt-HG-FP) MMBS

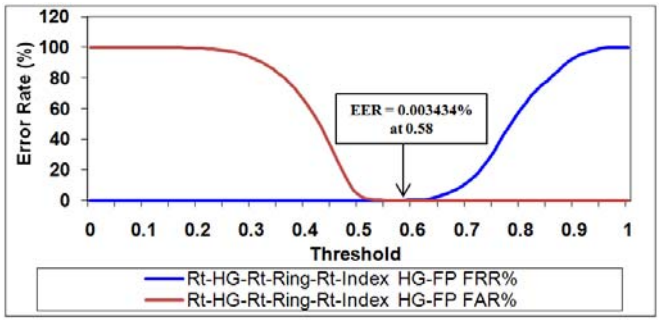

Fig. 18 FAR versus FRR and extracted EER for Rt-HG-FP MMBS

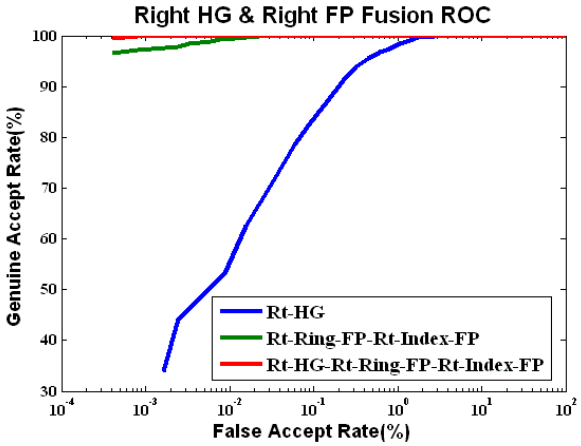

Fig. 19 ROC curves for Rt-HG-FP MMBS versus its constituents

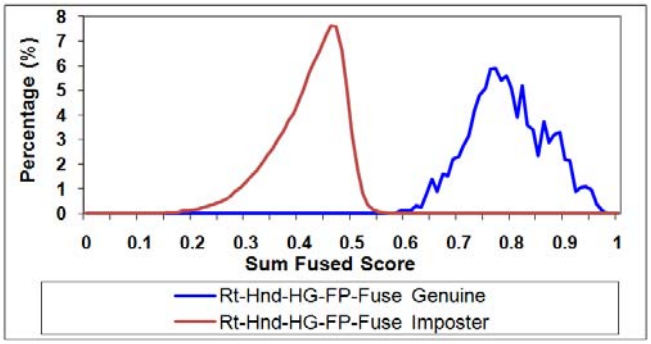

Fig. 20 Identification test for genuine and imposter sum fused score distributions of Rt-HG-FP MMBS

B. Lt-HG-FP Multimodal Biometric System

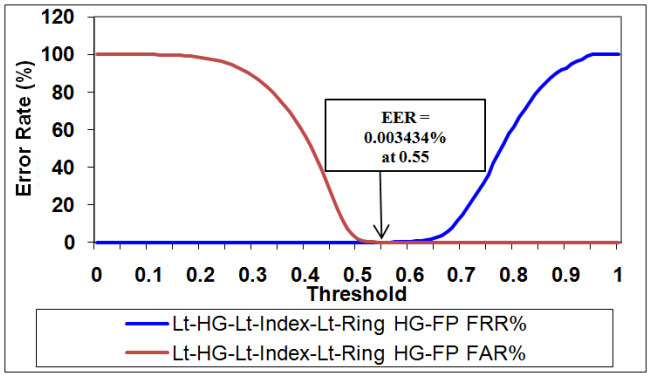

Fig. 21 FAR versus FRR and extracted EER for Lt-HG-FP MMBS

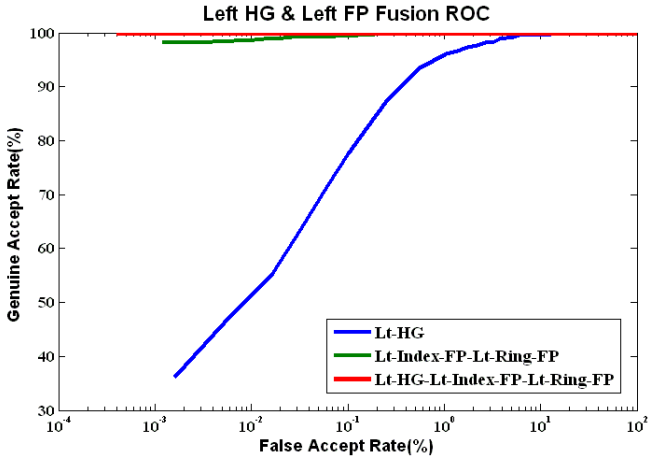

Fig. 22 ROC curves for Lt-HG-FP MMBS versus its constituents

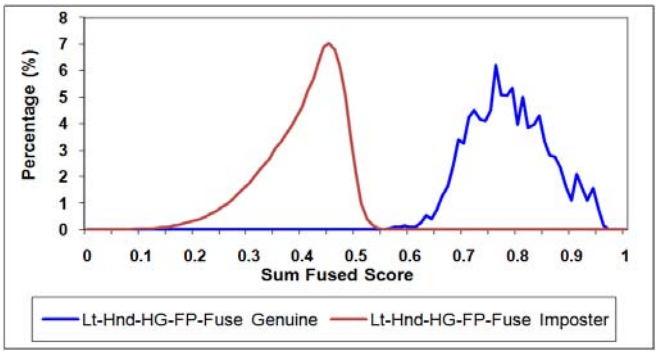

Fig. 23 Identification test for genuine and imposter sum fused score distributions of Lt-HG-FP MMBS

C. Rt-Lt-HG-FP Multimodal Biometric System

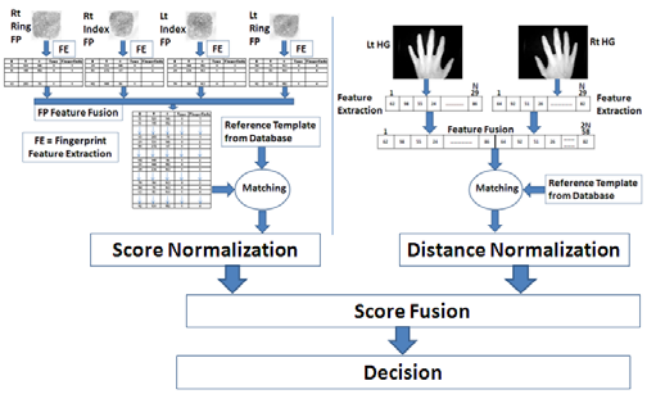

Fig. 24 Schematic for Rt-Lt-HG-FP MMBS

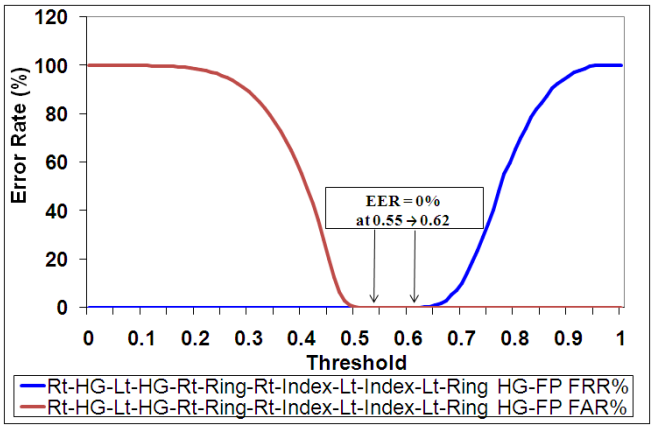

Fig. 25 Extracted EER for our Rt-Lt-HG-FP MMBS

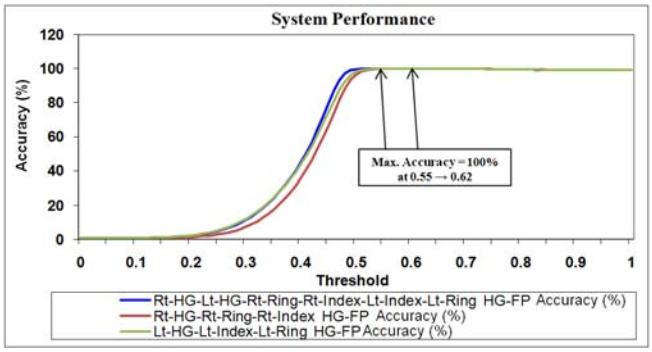

Fig. 26 Comparison between the accuracy for Rt-HG-FP, Lt-HG-FP, and Rt-Lt-HG-FP MMBSs

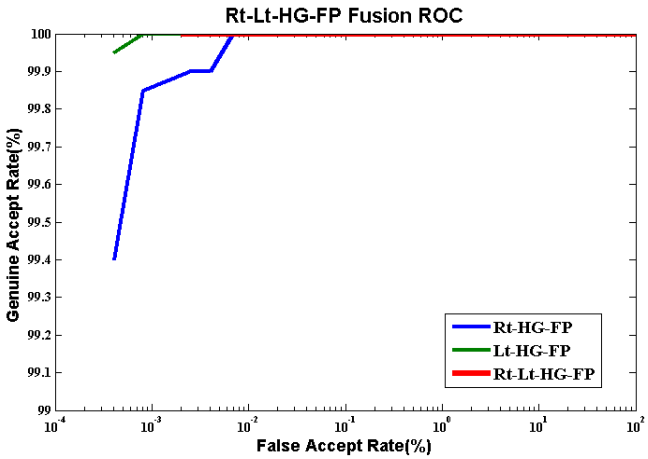

Fig. 27 ROC curves for Rt-Lt-HG-FP MMBS versus its constituents

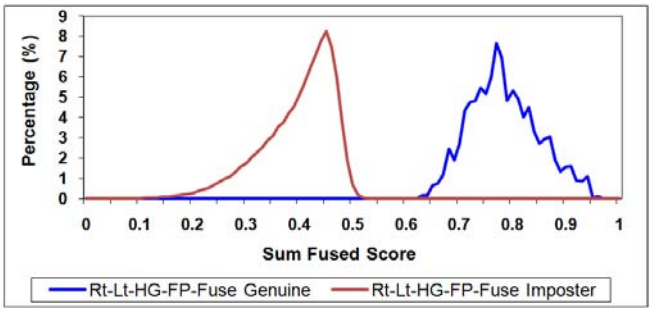

Fig. 28 Identification test for genuine and imposter sum fused score distributions of Rt-Lt-HG-FP MMBS

TABLE II
QUANTITATIVE PERFORMANCE COMPARISON BETWEEN OUR SINGLE-MODALITY HG & FP, BI-INSTANCE HG & FP, MULTI-INSTANCE FP, MULTIMODAL RT-HG-FP, MULTIMODAL LT-HG-FP, AND MULTIMODAL RT-LT-HG-FP BIOMETRIC SYSTEMS, AT CORRESPONDING THRESHOLD BETWEEN [.].

Modality	FAR%	FRR%	Accuracy%	TER%	EER%
HG Single-Modalities					
Rt-HG	0.091313	17.10	99.772345 [0.018]	*2.169293 [0.027]*	*1.192525 [0.026]*
Lt-HG	0.101010	22.50	99.719439 [0.018]	*4.384950 [0.026]*	*2.285051 [0.027]*
FP Single-Modalities					
Rt-Ring-FP	0.030707	9.40	99.894188 [42%]	*1.557172 [30%]*	*0.778586 [30%]*
Rt-Index-FP	0.018182	6.70	99.928257 [41%]	*0.928889 [28%]*	*0.658636 [30%]*
Lt-Index-FP	0.029899	7.30	99.911824 [39%]	*1.417071 [27%]*	*0.752020 [28%]*
Lt-Ring-FP	0.008081	6.00	99.943888 [37%]	*0.788384 [26%]*	*0.414141 [25%]*
HG Feature Fusion					
Rt-Lt-HG	0.016162	7.15	99.926653 [0.02]	*1.015758 [0.027]*	*0.507879 [0.027]*
HG Score Sum-Rule Fusion					
Rt-Lt-HG	0.040000	4.5	99.924248 [0.042]	*1.041919 [0.051]*	*0.541919 [0.053]*
HG Score Multiply-Rule Fusion					
Rt-Lt-HG	0.038384	4.65	99.924649 [0.004]	*1.377575 [0.007]*	*0.688789 [0.007]*
FP Biometric Feature Fusion					
Rt-FP	0.007677	0.70	99.986774 [34%]	*0.112323 [27%]*	*0.089798 [28%]*
Lt-FP	0.001211	0.80	99.992385 [34%]	*0.026667 [28%]*	*0.013333 [28%]*
Rt-Lt-FP	0.000404	0.05	99.999198 [35%]	*0.0020202 [34%]*	*0.001010 [34%]*
FP Score Sum-Rule Fusion					
Rt-FP	0.005660	1.15	99.985170 [39%]	*0.160808 [32%]*	*0.094242 [33%]*
Lt-FP	0.003230	0.80	99.990380 [34%]	*0.1624242 [28%]*	*0.121515 [30%]*
Rt-Lt-FP	0.000000	0.20	99.998397 [35%]	*0.0028283 [33%]*	*0.001414 [33%]*
Rt-HG-FP Score Fusion					
Rt-HG-FP	0.000808	0.30	99.996794 [0.61]	*0.006868 [0.58]*	*0.003434 [0.58]*
Lt-HG-FP Score Fusion					
Lt-HG-FP	0.000808	0.25	99.997194 [0.58]	*0.006868 [0.55]*	*0.003434 [0.55]*
Rt-Lt-HG-FP Score Fusion					
Rt-Lt-HG-FP	0.000000	0.00	100.00 [0.55-0.62]	*0.00 [0.55-0.62]*	*0.00 [0.55-0.62]*

D. Comparison Table between Our Proposed MMBS and Related Systems

TABLE III
COMPARISON OF DIFFERENT MMBSS DISCUSSED IN PRIOR RELATED WORK WITH OUR PROPOSED SYSTEM.

MMBS	Biometric Identifiers	Fusion Level and approaches	EER or other published performance	Testing Database size	Experimental Acquisition Setup
Rowe *et al.* [24]	Hand Shape, Fingerprint and Palmprint	Score-level fusion: sum-rule method	GAR=91.5% at FAR=0.01 fusing the palmprints for the 2 hands; not from fusing the 3 modalities	Experimentally 50 Persons	Yes
Kumar *et al.* [17]	Hand Shape, Palm Texture, and Fingerprint	Score-level fusion: using sum rule	EER=3.53%	Virtual 100 Persons as discussed in prior work section	Partially, FP is from different database
Nandakumar *et al.* [20]	Minutiae-based and texture-based Fingerprint	Match score, Quality Weighted Sum rule (QWS)	3.39%	MCYT [33] database of 750 FP, 10 per finger	No
Wei *et al.* [30]	Palmprint and Hand Geometry	Feature-level fusion	Accuracy =99.36%	Experimentally 51 Persons	Yes
Wu *et al.* [31]	Fusion of Phase and Orientation for Palmprint	Feature-level fusion	0.31%	Experimentally 392 different palmprints	Yes
Zhu *et al.* [32]	Finger Geometry, Knuckle print and Palmprint	coarse-to-fine hierarchical decision-level AND rule fusion	FRR=0.00898 at FAR=2.52e-6	Experimentally 190 persons	Yes
Cui *et al.* [5]	Face and Iris	Feature-level fusion	Accuracy for random choose ranged from 88.7% to 100%	Virtual multimodal database of 40 persons	No
Monwar *et al.* [9]	Face, Ear, and Signature (only system to include physical and behavioral characteristics)	Rank-level fusion: Logistic regression	1.12%	Virtual multimodal database of 40 persons	No
Sim *et al.* [27]	Continuous verification using face and Fingerprint	Holistic fusion	New TCR, PTCR, and usability measures proposed	Experimentally several users for each, 1000FP and 500 Face images	Yes
Snelick *et al.* [28]	Face and Fingerprint	Score level fusion: Max-score on quadric-linequadric normalized scores	0.63%	Virtual 972 persons, 2FP and 2 frontal face from FERET database[52]	No
Current System	Whole Hands Geometry and Fingerprint	Feature-level for similar traits and Transformation based score-level for HG&FP fusion	EER=*0.003434* for Lt or Rt HG+FP fusion and EER=0 for fusion of Lt and Rt HG+FP	Experimentally 100 Persons with high quality images of designed prototype	Yes

E. Computation Times Table for Different Proposed Single and MMBSs

TABLE IV
COMPUTATION TIMES CALCULATED FOR 300H X 300W FP IMAGES AND 320W X 240H HG IMAGES, CALCULATION WAS BASED ON: INTEL CELERON 2 GHZ CPU, 512 MBYTES OF RAMS.

Operation	Average Time	Programming Language Implementation
Single FP Enhancement	3 Sec.	MATLAB (slow interpreter than C++ compiler)
Single FP Feature Extraction	0.125 Sec.	MS VC++
1:1 FP Matching	0.15 Sec.	MS VC++
1:500 FP Matching	66 Sec.	MS VC++
1:1 2-Fused FPs Matching	0.27 Sec.	MS VC++
1:1 4-Fused FPs Matching	0.49 Sec.	MS VC++
Single HG Processing and Feature Extraction	3 mSec.	MS VC++
1:1 HG Matching	1 mSec	MS VC++
1:500 HG Matching	0.7 Sec.	MS VC++

VI. DISSCUSION

The main advantages of our prototype design is its compactness, low cost (using on the shelf components as NIR CCD of 40$ and FP chips of 50$ each per single finger which can be cheaper if more chips are used), user convenience (single or double hands landings), and acquisition of more than single biometric trait in single or double user interactions. As practical biometric system is all about a trade-off between individuality and usability, and is mainly specified by the level of security (low-medium-high) required [2], [6], [11], [25], we attempted to optimize both by selecting unique biometric features and its easy usability in one system design for a whole hands FP and NIR dorsal HG MMBS. In addition to the previous merits, its high performance may make it a candidate to various security levels systems, from low security level like in most time-attendance control systems to border control high security and e-passports. A one practical merit for our hardware prototype design is its modularity, we can use it for single user maneuver acquisition for HG+FP, or we can use either FP PCB or freestyle platen alone to implement a multi-instance FP or HG system with main advantages of: (a) High accuracy through multiple independent FP instances from different fingers for the same user, and (b) User convenience (i.e. scan 2 FP instances as the same way of a single FP).

The single modality-FP systems that rely on such small size sensors (0.6”X0.6”) can only target simple applications like employee time attendance. Our 2-instance HG and 4-instance FP system showed high accuracy and can be used for higher level security applications like accessing secure resources [27]. This fact was evidenced from the increase of accuracy (with our high quality images) from single-modality, 2-instances, and finally to 4-instances FP MMBS.

It is evident that the price for any solid-state FP sensor is one-tenth its equivalent optical scanner. Furthermore, the capacitive sensor is very compact in its size, normally a surface mount IC package. The main drawback for most capacitive FP scanners is its small image array size and short durability. Our FP chips have size of 0.6”X0.6”. Any FP matching algorithm must rely only on the local FP features (i.e. minutia points) to be used for matching on such small size images. It is well-known that when we fuse medium-size FP instances from different user fingers can lead to better results than acquiring a large size one instance FP. Multiple instances ensure the validity of identity based on multiple evidences produced from different independent sources and will make it hard on fakers to do it for more than one FP. We soldered 2 FP sensors in the same PCB and on the same data bus for ease of single step acquisition. As we showed through this paper’s results, that the multiple FP instances fusion have a huge influence on the FP system accuracy. Another drawback of the HG module is its non-compactness due to focal length of the camera. It can be more compact with set of mirrors.

This work contributed the study of similarity between Rt and Lt NIR HG shapes for the same person. To our knowledge, the existing biometrics literature has never got benefits from both hands for enhancing the HG systems accuracy. Furthermore, the HG prototype system proposed in [51] and found in most commercial HG systems don’t support the left hand as they use pegs to control opening of fingers while we proposed solutions to that issue by freestyle prototypes [39], [43]-[45]. Also, most pegs controlled systems do not take thumb finger features into account while we considered it in our current prototype despite its discrimination power studied in [39].

We found similarity to some extent between the right and left HG for the same person (11%) and we can’t say the right hand features are similar to left hand (this is obvious for example in case of handball players “they use one hand most of the time to catch and throw the ball”). Hand geometry can change a bit with working conditions and adaptations (for right and left handed persons). So, we can’t average the Rt-HG with the Lt-HG (to consolidate the personal HG patterns) assuming that they are the same, as we proved this uniqueness through inter-personal and intra-personal studies. The previous published work in the literature always propose the concatenation of similar distances from different traits like: Geometrical distances of HG with distance measurements of face in addition to texture measurements of the palmprint. Our system is superior in the fusion of similar traits in a single feature vector, as we fused the Lt and Rt hands in one array to completely represent the personal HG pattern. The obtained result after fusing (Rt-Lt-HG system) is much better than Rt-HG or Lt-HG as a single modality.

Biometric systems that integrate information at an early stage of processing are believed to be more effective than those which perform integration at a later stage [8] and this is the case for our system. Furthermore, it is evident that the fusion at the feature vector levels is the powerful fusion methodologies due to some reasons: (a) Fusion at the sensor level contends with the presence of noise in the primary sensed data. (b) When we fuse at the feature level, we are sure that we fuse the genuine unique noise-free biometric data, which validate the identity based on multiple evidences acquired from different sources even if these sources are for similar biometric traits (e.g. Rt-Index-FP and Rt-Ring-FP). (c) After deploying the matcher stage, the data is drastically reduced and the only choice is to fuse them using this little available data.

We added a definition for minutiae fusion, collecting the minutiae from different FPs into a single feature file, and we added a new field (in addition to the classical X-Y-Θ-Type fields) called FingerCode, as a code for representing which finger of the person this minutia came from (1 for right ring, 2 for right index, 3 for left index, and 4 for left ring). We matched these minutiae with a single matcher (the output is 1 or 2 or 4 different matched graphs and a single similarity ratio). Fingerprint matching searches for 1 or 2 or 4 graphs instead of looking for just single one based on how many FingerCodes in the input minutiae file to let it matches different minutia points sources.

If the resultant FP and HG images that acquired in [16]-[18], [24] are compared qualitatively with our acquired images, these images are of lower quality compared to our NIR dorsal HG images acquired by low price NIR CCD

camera and FP images acquired by FPS200 FP capacitive sensors.

The results of fusion between HG&FP on the level of single hand is accurate (EER=*0.003434*) for both Rt/Lt hands as can be seen in Table II. Its main merit is the single user interaction with the system. This high accuracy may make these systems a candidate for med-high security applications. Furthermore, It is very hard to spoof a biometric system with these bi-instance HG and 4-instances FP arrangements. As can be seen from Fig. 28, our Rt-Lt-HG-FP MMBS was very accurate (EER=0 based on the 100 volunteers database size of high quality images shown in Fig. 3) and the identification genuine and imposter matching scores were not only separated on a single threshold but also through a range of score thresholds (0.55-0.62) that allow feasibility of system operability with expanded database size. Rt-Lt-HG-FP system validated our main objective through proving that: if more than one form of unique features were used to represent a single identity, the biometric system will robustly identify the individuals like human eyes (i.e. based on multiple evidences). We want to emphasize that these accurate results are based on our experimental dataset of 100 persons with high quality images acquired to both NIR dorsal HG and FP modalities [26]. As Nandakumar *et al.* [20] illustrated that with good quality images, the matcher performance can be very accurate and that is our Rt/Lt HG-FP MMBS case.

One interesting finding and coincidence in our quantitative analysis is that Lt-HG-FP EER is equal to that of Rt-HG-FP fusions (EER=*0.003434*, as in Table II and Figs. 18-23), with different corresponding optimal thresholds for EER and efficiencies. That is due to different combinations of Rt/Lt HG and FP features fused. The individuality power of Rt hand combined HG-FP features equal that of Lt hand. The practical impact of this finding is that, we can use (preselect at enrollment or when there is FTE) either right or left hand, in cases of persons with one hand cut due to accidents or persons who have one erased FP features in one hand (hard mechanical, chemical factories workers, and farmers), with no accuracy degradation (based on this high quality images database).

One of our merits in system design is its hardware modularity, for example, we can scan both Rt-Lt-HG-FP in one acquisition step if we simply doubled the used H/W (2 NIR CCD images and 4 FP sensors) and re-design the compact space to allow landing of the two hands together, that space can be even smaller and compact by rotating the right hand 45 degrees CCW and the left hand 45 degrees CW, as well the FP sensors and cameras can be also re-oriented at angles to save and minimize space. We compared our system to similar existing MMBs (to our knowledge) in Table III, with comparison basis of few 5 characteristics such as: types of modalities fused, fusion level and approach, EER or other performance measure as accuracy, testing database size, and whether these modalities in datasets belong to same subjects or virtually combined from different databases. Computation times were presented in Table IV based on a standard capability PC and the results based on this ordinary PC with 500MB RAMs (can be replaced by single board PC embedded with this prototype scanner unit) showed the timing and practical feasibility for a future optimization by an accelerated embedded fast hardware.

VII. CONCLUSIONS

An increasing number of biometrics-based identification and verification systems, which are deployed for many civilian and forensic applications, are emerging. In recent years, hand has become a very popular access control biometrics (including fingerprints, palmprints, hand geometry, and hand veins), which has captured almost half of the commercial access control market.

In order to limit the tradeoffs of the unimodal biometric systems and for realizing a whole hand-based MMBS using fingerprint, hand geometry, and hand vein, our system was designed in 2008 with all these tradeoffs [26] in mind. The proposed MMBS was built to tackle the tradeoffs found in unimodal systems, and for its usage in med-high security applications. A sample database of 3000 different images belonging to 100 volunteers was collected. We captured 30 images per person (5 Rt Ring FP, 5 Rt Index FP, 5Lt Index FP, 5 Lt Ring FP, 5 Rt HG, and 5 Lt HG). The database consisted of 2000 fingerprint images and 1000 hand shape images. Each volunteer provided FP and HG biometric traits with a written consent.

We discussed how we obtained a single decision about the identity for the user from multiple biometric traits. First, we showed how we fused the Rt and Lt HG features in a single feature vector to represent and validates the user identity. Second, we illustrated how we fused the minutia lists originating from different fingers for the same person. Finally, we showed how we normalized and fused different biometric modalities (HG and FP) using the Min-Max score normalization method and the sum-of-scores fusion technique. The important analysis that was experimentally emphasized in this paper is, what is the effect of biometric feature and score levels fusion on the accuracy of the HG-FP biometric system?.

Results of our single and whole hands showed an accurate performance for our systems. Our future work include adding the analysis of hand vein (HV) pattern that was implemented in [35], [47] and was added to our prototype into our current proposed bi-modalities (HG-FP), to achieve with this tri-modalities even a much better performance with single a acquisition steps. The proposed acquisition prototype is able to acquire the NIR dorsal hand vein patterns with shown preliminary images acquisition results in [26]. We are currently collecting a dataset of 100 HV patterns (5 for each Lt and Rt hands) belonging to the same enrolled volunteers under the same acquisition standard protocol. One final future work to our current systems is a combined HG-FP-HV feature selection stage prior to feature fusion (as a continuation to our HG features discrimination power conducted in [39], [45]), for all our current (HG-FP) and our added future modality (HV).

ACKNOWLEDGMENT

Biomedical technician staff members of Suez Canal Authority Hospital are acknowledged for their suggestions in building the prototype, thanks to Mr. Sobhy Refaat and Mr. Ibrahim Hemdan for their suggestions. Authors would like to acknowledge Mr. Mohamed Zaki for his assistance in fabricating the PCB for our fingerprint acquisition system.

REFERENCES

[1] S. Pankanti, S. Prabhakar, and A. K. Jain, "On the individuality of fingerprints," *IEEE Transactions on Pattern Analysis and Machine Intelligence*, vol. 24, pp. 1010-1025, 2002.

[2] A. K. Jain, A. Ross, and S. Prabhakar, "An introduction to biometric recognition," *IEEE Transactions on Circuits and Systems for Video Technology, Special Issue on Image- and Video-Based Biometrics*, vol. 14, pp. 4-21, January 2004.

[3] M. Golfarelli, D. Maio, and D. Maltoni, "On the error-reject tradeoff in biometric verification systems," *IEEE Trans. on Pattern Anal. and Mach. Intell.*, vol. 19, pp. 786–796, July 1997.

[4] A. Ross and A. K. Jain, "Multimodal biometrics: An overview," *Proc. of 12th European Signal Processing Conference (EUSIPCO), Vienna, Austria*, pp. 1221-1224, September 2004.

[5] J. Cui, J. P. Li, and X. J. Lu, "Study on multi-Biometric feature fusion and recognition model," *Proc. of International Conference on Apperceiving Computing and Intelligence Analysis (ICACIA), Chengdu, China*, pp. 66-69, 2009.

[6] A. K. Jain, "Biometric recognition: Overview and recent advances," *Progress in Pattern Recognition, Image Analysis and Applications*, pp. 13-19, 2007.

[7] D. Maltoni, D. Maio, A. K. Jain, and S. Prabhakar, "Handbook of fingerprint recognition," *Springer-Verlag*, 2003.

[8] V. M. Mane and D. V. Jadhav, "Review of multimodal biometrics: Applications, challenges and research areas," *Int. Journal of Biometrics and Bioinformatics (IJBB)*, vol. 3, 2009.

[9] M. M. Monwar and M. L. Gavrilova, "Multimodal biometric system using rank-level fusion approach," *IEEE Transactions on Systems Man and Cybernetics Part B (Cybernetics)*, vol. 39, pp. 867-878, 2009.

[10] A. Ross and A. K. Jain, "Information fusion in biometrics," *Pattern Recognition Letters*, vol. 24, pp. 2115–2125, Sep. 2003.

[11] A. Ross, K. Nandakumar, and A. K. Jain, "Handbook of multibiometrics," *New York: Springer-Verlag*, 2006.

[12] M. F. Zanuy, J. F. Aguilar, J. O. Garcia, and J. G. Rodriguez, "Multimodal biometric databases: An overview," *Conference Report, IEEE 39th International Carnahan Conf. on Security Technology, Las Palmas de Gran Canary, Spain*, October 2005.

[13] K. W. Bowyer, K. I. Chang, P. Yan, P. J. Flynn, E. Hansley, and S. Sarkar, "Multi-modal biometrics: An overview," *2nd Workshop on Multi-Modal User Authentication, France.*, 2006.

[14] A. K. Jain and A. Ross, "Fingerprint mosaicking," *IEEE International Conference on Acoustics, Speech, and Signal Processing, Orlando, USA*, vol. 4, pp. 4064-4067, 2002.

[15] T. Kinnunen, V. Hautamaki, and P. Franti, "Fusion of spectral feature sets for accurate speaker identification," *Proc. of 9th Conf. Speech Comput., Russia*, pp. 361-365, 2004.

[16] A. Kumar, D. C. M. Wong, H. C. Shen, and A. K. Jain, "Personal verification using palmprint and hand geometry biometric," *in Audio- and Video-Based Biometric Person Authentication.* vol. 2688, ed: Springer Berlin Heidelberg, 2003, pp. 668-678.

[17] A. Kumar and D. Zhang, "Combining fingerprint, palmprint and hand-shape for user authentication," *Proc. of International Conference of Pattern Recognition (ICPR)*, pp. 549-552, 2006.

[18] A. Kumar and D. Zhang, "Personal recognition using hand shape and texture," *IEEE Trans. on Image Processing*, vol. 15, pp. 2454-2461, August 2006.

[19] K. Nandakumar, A. K. Jain, and A. Ross, "Fusion in Multibiometric identification systems: What about the missing data?" *Proc. of the 3rd IAPR/IEEE International Conference on Biometrics (ICB), Alghero, Italy*, June 2009.

[20] K. Nandakumar, A. Ross, and A. K. Jain, "Incorporating ancillary information in multibiometric systems," *Handbook of Biometrics. New York: Springer-Verlag*, pp. 335–355, 2007.

[21] N. Poh and S. Bengio, "How do correlation and variance of base-experts affect fusion in biometric authentication tasks?," *IEEE Transactions on Signal Processing*, vol. 53, pp. 4384-4396, 2005.

[22] S. Ribaric and I. Fratric, "Experimental evaluation of matching-score normalization techniques on different multimodal biometric systems," *IEEE MELECON, Malaga, Spain*, 2006.

[23] A. Ross and R. Govindarajan, "Feature level fusion using hand and face biometrics," *Proc. of SPIE Conference on Biometric Technology for Human Identification II, Orlando, USA*, vol. 5779, pp. 196-204, 2005.

[24] R. K. Rowe, U. Uludag, M. Demirkus, S. Parthasaradhi, and A. K. Jain, "A multispectral whole-hand biometric authentication system," *Proc. of Biometric Symposium, Biometric Consortium Conference, Baltimore*, September 2007.

[25] B. Schouten and B. Jacobs, "Biometrics and their use in e-passports," *Image and Vision Computing*, vol. 27, pp. 305-312, February 2009.

[26] M. K. Shahin, A. M. Badawi, and M. E. Rasmy, "A multimodal hand vein, hand geometry, and fingerprint prototype design for high security biometrics," *Proc. of 4th IEEE Cairo Int. Biomedical Engineering Conf. (CIBEC2008), Egypt*, Dec. 2008.

[27] T. Sim, S. Zhang, R. Janakiraman, and S. Kumar, "Continuous verification using multimodal biometrics," *IEEE Transactions on Pattern Analysis and Machine Intelligence*, vol. 29, pp. 687-700, 2007.

[28] R. Snelick, U. Uludag, A. Mink, M. Indovina, and A. K. Jain, "Large-scale evaluation of multimodal biometric authentication using state-of-the-art systems," *IEEE Transactions on Pattern Analysis and Machine Intelligence*, vol. 27, pp. 450-455, 2005.

[29] K. A. Toh, "Error-rate based biometrics fusion," *S.W. Lee and S.Z. Li (Eds): ICB 2007, LNCS, Springer-Verlag Berlin/Heidelberg*, vol. 4642, pp. 191-200, 2007.

[30] X. Y. Wei, D. Xu, and C. W. Ngo, "Multibiometrics based on palmprint and hand geometry," *Proc. of 4th International Conf. on Computer and Information Science (ICIS'05)*, 2005.

[31] X. Wu, K. Wang, F. Zhang, and D. Zhang, "Fusion of phase and orientation information for palmprint authentication," *Proc. of Int. Conf. on Image Processing (ICIP)*, September 2005.

[32] L. Q. Zhu and S. Y. Zhang, "Multimodal biometric identification system based on finger geometry, knuckle print, and palm print," *Pattern Recog. Letters*, On-Line, June 2010.

[33] J. Ortega-Garcia, J. Fierrez-Aguilar, D. Simon, J. Gonzalez-Rodriguez, M. Faundez, V. Espinosa, A. Satue, I. Hernaez, J. J. Igarza, C. Vivaracho, D. Escudero, and Q. I. Moro, "MCYT baseline corpus: A bimodal biometric database," *IEE Proc. on Vision, Image and Signal Proc., Special Issue on Biometrics on the Internet*, vol. 150, pp. 395-401, December, 2003.

[34] M. K. Shahin, A. M. Badawi, and M. S. Kamel, "Biometric authentication using fast correlation of hand vein patterns," *Proc. of 3rd IEEE Cairo International Biomedical Engineering Conference (CIBEC06), Cairo, Egypt*, December 2006.

[35] M. K. Shahin, A. M. Badawi, and M. S. Kamel, "Biometric authentication using fast correlation of near infrared hand vein patterns," *International Journal of Biological and Life Sciences*, vol. 2, pp. 141-148, 2007.

[36] J. Egan, "Signal detection theory and ROC analysis," *Academic Press, New York*, 1975.

[37] http://www.securityfocus.com/news/6717, Accessed June 2006.

[38] H. Chen, H. Valizadegan, C. Jackson, S. Soltysiak, and A. K. Jain, "Fake hands: Spoofing hand geometry systems," *Biometric Consortium, Washington DC*, September 2005.

[39] N. Abd-El-Rahman, "A prototype of automatic hand geometry verification system," *Master Thesis, Cairo University, Faculty of Engineering, Systems and Biomedical Dept.*, 2002.

[40] M. K. Shahin, A. M. Badawi, and M. S. kamel, "On-line, low-cost and PC-based fingerprint verification system based on solid-state capacitance sensor," *Proc. of IEEE International Conference on Industrial Electronics, Technology and Automation (IETA2001),Cairo Egypt*, December 2001.
[41] http://www.veridicom.com/, Accessed January 2005.
[42] http://www.elexol.com/, Accessed April 2006.
[43] A. Badawi and M. Kamel, "Freestyle hand geometry verification system," *Proc. of 46th IEEE Midwest Symposium on circuits and systems*, 2003.
[44] A. M. Badawi, S. A. El-Naggar, and M. S. Kamel, "Freestyle non-guided true-anatomical biometrics: A fusion of hand geometry and texture features," *Proc. of 3rd IEEE Cairo Int. Biomedical Engineering Conf. (CIBEC2006), Cairo, Eygpt*, December 2006.
[45] S. El-Naggar, "Freestyle hand biometric system based on geometry and texture features," *Master Thesis, Cairo Univ., Faculty of Engineering, Systems and Biomedical Dept.*, 2005.
[46] A. M. Badawi and M. K. Shahin, "Frequency domain spectral hand vein patterns authentication," *Proc. of 3rd IEEE Cairo Int. Biomedical Engineering Conf. (CIBEC2006), Egypt*, December 2006.
[47] M. K. Shahin, "Hand vein based biometric verification system," *Master Thesis, Cairo University, Faculty of Engineering, Systems and Biomedical Dept.*, 2005.
[48] S. Chikkerur, "Online fingerprint verification system," *Master Thesis, the State University of New York at Buffalo*, 2005.
[49] C. I. Watson, M. D. Garris, E. Tabassi, C. L. Wilson, R. M. McCabe, S. Janet, and K. Ko, "User's guide to NIST biometric image software (NBIS)," *Technical Report National Institute of Standards and Technology*, 2008.
[50] S. Chikkerur, A. N. Cartwright, and V. Govindaraju, "K-plet and coupled BFS: A graph based fingerprint representation and matching algorithm," *International Conference on Biometrics (ICB)*, pp. 309-315, 2006.
[51] A. K. Jain, A. Ross, and S. Pankanti, "A prototype Hand geometry-based verification system," *Proc. of 2nd International Conference on Audio- and Video-based Biometric Person Authentication, Washington D.C.*, pp. 166-171, March 1999.
[52] "The Facial Recognition Technology (FERET) Database," http://www.itl.nist.gov/iad/humanid/feret/feret_master.html, 2004.

Mohamed Khairy Shahin received his B.Sc. and M.Sc. in 2000, and 2005 from Department of Systems & Biomedical Engineering (SBME), Cairo University, Egypt. He worked as a Biomedical Design Engineer in the 3D Ultrasonography project at International Biomedical Electronics (IBE), R&D Division, BAHGAT Group from 2000 to 2003. He is a Senior Biomedical Engineer, Suez Canal Authority Hospital, Ismaillia, Egypt since June 2003. He was a Head of Biomedical Engineering Program at Ideal Academy for Health Training, Kingdom of Saudia Aribia from March 2009 to June 2010, while he was on leave of Suez Canal Authority. His research interests are in Pattern Recognition, Image Processing, and Biometrics. He is currently a Ph.D. student at Department of Systems & Biomedical Engineering, Cairo University, Egypt, under supervision of Dr. Ahmed M. Badawi and Dr. Mohamed E. M. Rasmy.

Ahmed Mohamed Badawi (M'05-SM'06) received his B.Sc., M.Sc., Ph.D. in 1990, 1993, and 1996 respectively from Department of Systems & Biomedical Engineering, Cairo University.
He was an assistant professor, associate professor, and full professor in 1996, 2001, and 2007 respectively at Systems & Biomedical Engineering Cairo University. He is a professor at Systems & Biomedical Engineering, Cairo University. His research interests are in Medical Imaging, 3D/4D Ultrasound Scanning, Reconstruction, Visualization, and Measurements, 4D Surgical Navigation, Image Processing, Computer Vision and Pattern Recognition in Medicine, Neural Networks, Fuzzy Systems, Medical Classification, Biometrics, Intelligent Medical Systems, and Medical Software Workstations. He is a reviewer of several international journals, chairman of several international conferences sessions and track chairman.
Dr. Badawi is a senior member, IEEE, a member in IEEE Engineering in Medicine and Biology society. Dr. Badawi published over 75 papers in journals and peer reviewed conferences. He awarded several prestigious awards such as Egyptian National Academy for Scientific Research and Technology, Cairo University award for Engineering Research. Dr. Badawi was a director of Imaging Solutions Department at ibetech.com where he was the head of the team who developed the first 3D ultrasound system in Egypt. Dr. Badawi has over 20 years experience in Systems & Biomedical Engineering teaching and research. Dr. Badawi supervised over 15 M.Sc. and 2 Ph.D. students.

Mohamed Emad Mousa Rasmy was born in Cairo, Egypt in 1943. He received the B.Sc. and M.Sc. in Electrical Engineering from Cairo University in 1964, and 1968, and M.Sc. in applied mathematics and Ph.D. in Electrical Engineering from Calgary University in 1971 and 1974, respectively. Since 1976, he has been with the Systems and Biomedical Engineering Department of Cairo University where he is currently an Emeritus Professor. His research interests include modeling and simulation, control systems, image and signal processing.